Activation of C_2H_6, C_3H_8, and c-C_3H_6 by Gas-Phase Zr^+ and the Thermochemistry of Zr−Ligand Complexes

Michael R. Sievers† and P. B. Armentrout*

Department of Chemistry, University of Utah, Salt Lake City, Utah 84112

Received January 14, 2003

The kinetic energy dependences of the reactions of Zr^+ (^4F) with ethane, propane, and cyclopropane have been studied using guided ion beam mass spectrometry. It is found that dehydrogenation is efficient and the dominant process at low energies in all three reaction systems. Efficient C−C bond activation is also observed at low energies in the cyclopropane system. At high energies, products resulting from both C−H and C−C cleavage processes are appreciable for all three hydrocarbon systems. The observation of dihydride and hydridomethyl zirconium cation products provides insight into the reaction mechanisms operating in these processes. The results for Zr^+ are compared with those for the first-row transition metal congener Ti^+ and the differences in behavior and mechanism discussed. Modeling of the endothermic reaction cross sections yields the 0 K bond dissociation energies (in eV) of $D_0(Zr^+-2H) = 5.02 \pm 0.13$, $D_0(Zr^+-C) = 4.62 \pm 0.16$, $D_0(Zr^+-CH) = 5.89 \pm 0.13$, $D_0(Zr^+-CH_2) = 4.61 \pm 0.05$, $D_0(Zr^+-CH_3) = 2.36 \pm 0.10$, $D_0[Zr^+-(H)(CH_3)] = 5.43 \pm 0.15$, $D_0(Zr^+-C_2H) = 4.57 \pm 0.12$, $D_0(Zr^+-C_2H_2) = 2.83 \pm 0.15$, $D_0(Zr^+-C_2H_3) = 3.78 \pm 0.24$, $D_0(Zr^+-C_2H_4) = 2.84 \pm 0.18$, $D_0(Zr^+-C_2H_5) = 2.37 \pm 0.17$, $D_0(Zr^+-C_3H_2) = 5.45 \pm 0.20$, and $D_0(Zr^+-C_3H_3) \geq 4.10 \pm 0.23$. The observation of exothermic processes sets lower limits for the bond energies of Zr^+ to propyne and propene of 2.84 and 1.22 eV, respectively.

Downloaded by CARLI CONSORTIUM on June 29, 2009
Published on May 23, 2003 on http://pubs.acs.org | doi: 10.1021/om030028u

Introduction

As part of a long-term project in our laboratory, we are interested in examining periodic trends in the reactions of transition metal ions (M^+) with small hydrocarbons. Extensive work for first-row transition metal elements has revealed the electronic requirements for the activation of C−H and C−C bonds at metal centers[1−4] and provided an examination of the periodic trends in such reactivity unavailable in condensed-phase media.[1,5] A particular interest in our research is to use guided ion beam methods to obtain metal−hydrogen and metal−carbon bond dissociation energies (BDEs).[6−10] Such thermochemistry is of obvious fundamental interest and also has implications in understanding a variety of catalytic reactions involving transition metal systems.[11] We have recently extended our studies to the reactivity of second-row transition metal cations with small hydrocarbons. This now includes work on Y^+,[12,13] Nb^+,[14] Ru^+,[15] Rh^+,[16,17] Pd^+,[18] and Ag^+,[19] and a review.[20] Recently, we examined the reactions of Zr^+ with methane in a comprehensive experimental and theoretical study.[21]

In the present study, we extend this work to examine Zr^+ and describe its reactions with ethane, propane, and cyclopropane. The alkane systems have been examined at thermal energies by Ranasinghe, McMahon, and Freiser[22] using ion cyclotron resonance (ICR) mass spectrometry. Consequently, only exothermic processes were examined. Dehydrogenations (and in some cases, double dehydrogenations) were found to be the major reactions

† Present address: IBM, Yorktown Heights, NY.

(1) For reviews, see: Armentrout, P. B. In *Selective Hydrocarbon Activation: Principles and Progress*; Davies, J. A., Watson, P. L., Greenberg, A., Liebman, J. F., Eds.; VCH: New York, 1990; p 467. Armentrout, P. B. In *Gas-Phase Inorganic Chemistry*; Russell, D. H., Ed.; Plenum: New York, 1989; p 1. Armentrout, P. B.; Beauchamp, J. L. *Acc. Chem. Res.* **1989**, *22*, 315.

(2) Armentrout, P. B. *Science* **1991**, *251*, 175. Armentrout, P. B. *Annu. Rev. Phys. Chem.* **1990**, *41*, 313.

(3) Weisshaar, J. C. *Adv. Chem. Phys.* **1992**, *82*, 213. Weisshaar, J. C. *Acc. Chem. Res.* **1993**, *26*, 213.

(4) van Koppen, P. A. M.; Kemper, P. R.; Bowers, M. T. *J. Am. Chem. Soc.* **1992**, *114*, 1083, 10941. van Koppen, P. A. M.; Kemper, P. R.; Bowers, M. T. In *Organometallic Ion Chemistry*; Freiser, B. S., Ed.; Kluwer: Dordrecht, 1995; pp 157−196.

(5) Allison, J. *Prog. Inorg. Chem.* **1986**, *34*, 627. Squires, R. R. *Chem. Rev.* **1987**, *87*, 623. *Gas-Phase Inorganic Chemistry*; Russell, D. H., Ed.; Plenum: New York, 1989. Eller, K.; Schwarz, H. *Chem. Rev.* **1991**, *91*, 1121.

(6) Armentrout, P. B.; Georgiadis, R. *Polyhedron* 1988, *7*, 1573.

(7) Armentrout, P. B. *ACS Symp. Ser.* **1990**, *428*, 18.

(8) Armentrout, P. B.; Clemmer, D. E. In *Energetics of Organometallic Species*; Simoes, J. A. M., Beauchamp, J. L., Eds.; Kluwer: Dordrecht, 1992; p 321.

(9) Armentrout, P. B.; Kickel, B. L. In *Organometallic Ion Chemistry*, Freiser, B. S., Ed.; Kluwer: Dordrecht, 1995; pp 1−45.

(10) *Organometallic Ion Chemistry*, Freiser, B. S., Ed.; Kluwer: Dordrecht, 1995.

(11) Crabtree, R. H. *Chem. Rev.* **1985**, *85*, 245.

(12) Sunderlin, L. S.; Armentrout, P. B. *J. Am. Chem. Soc.* **1989**, *111*, 3845.

(13) Kickel, B. L.; Armentrout, P. B. *J. Am. Chem. Soc.* **1995**, *117*, 4057.

(14) Sievers, M. R.; Chen, Y.-M.; Haynes, C. L.; Armentrout, P. B. *Int. J. Mass Spectrom.* **2000**, *195/196*, 149.

(15) Armentrout, P. B.; Chen, Y.-M. *J. Am. Soc. Mass Spectrom.* **1999**, *10*, 821.

(16) Chen, Y.-M.; Armentrout, P. B. *J. Phys. Chem.* **1995**, *99*, 10775.

(17) Chen, Y.-M.; Armentrout, P. B. *J. Am. Chem. Soc.* **1995**, *117*, 9291.

(18) Chen, Y.-M.; Sievers, M. R.; Armentrout, P. B. *Int. J. Mass Spectrom. Ion Processes* **1997**, *167/168*, 195.

(19) Chen, Y.-M.; Armentrout, P. B. *J. Phys. Chem.* **1995**, *99*, 11424.

(20) Armentrout, P. B. *Organometallic Bonding and Reactivity*; Brown, J. M., Hofmann, P., Eds.; Topics in Organometallic Chemistry, Vol. 4; Springer-Verlag: Berlin, 1999; pp 1−45.

(21) Armentrout, P. B.; Sievers, M. R. *J. Phys. Chem. A*, in press.

(22) Ranasinghe, Y. A.; MacMahon, T. J.; Freiser, B. S. *J. Phys. Chem.* **1991**, *95*, 7721.

10.1021/om030028u CCC: $25.00 © 2003 American Chemical Society
Publication on Web 05/23/2003

Table 1. Zr^+-L Bond Energies (eV) at 0 K

	this work	previous work	
species	experiment	experiment	theory
Zr^+-H		2.26 (0.08)[a]	2.37,[b] 2.46,[c] 2.46,[d] 2.56,[e] 2.55[f]
Zr^+-2H	5.02 (0.13)	5.11 (0.01)[g]	5.20,[g] 5.15[g]
Zr^+-C	4.62 (0.16)	4.72 (0.11)[h]	4.60[f]
Zr^+-CH	5.89 (0.13)	5.96(0.22)[f]	5.50[f]
Zr^+-CH_2	4.61 (0.05)	4.62 (0.07)[f]	4.37,[f] 4.38(0.13),[i] 4.40[j]
Zr^+-CH_3	2.36 (0.10)	2.30 (0.24)[f]	2.80,[f] 2.48(0.13)[k]
Zr^+-(H)(CH_3)	5.43 (0.15)		5.37,[f] 5.70[l]
Zr^+-C_2H	4.57 (0.12)		
$Zr^+-C_2H_2$	2.83 (0.15)	2.56 (0.13)[m]	2.95[n]
$Zr^+-C_2H_3$	3.78 (0.24)		
$Zr^+-C_2H_4$	2.84 (0.18)		
$Zr^+-C_2H_5$	2.37 (0.17)		
$Zr^+-C_3H_2$	5.45 (0.20)		
$Zr^+-C_3H_3$	≥4.10 (0.23)		
$Zr^+-C_3H_4$	>2.84		
$Zr^+-C_3H_6$	>1.22		

[a] Ref 23. [b] Ref 27. [c] Ref 28. [d] Ref 29. [e] Ref 30. [f] Ref 21. [g] Ref 25. [h] Ref 24. [i] Ref 33. [j] Ref 32. [k] Ref 34. [l] Ref 35. [m] Ref 26. [n] Ref 37.

for the linear alkanes examined. Here, we are able to investigate the reactions of Zr^+ with these small, saturated hydrocarbons and cyclopropane over a wide range of kinetic energies, examining both endothermic and exothermic processes. This permits the extraction of systematic thermodynamic as well as mechanistic information.

There is relatively little thermochemistry available for zirconium species in the literature, as shown in Table 1. We have previously measured BDEs for Zr^+-H, Zr^+-C, and Zr^+-O by determining the endothermicities of the formation of these species from reactions of Zr^+ with H_2 (and D_2)[23] and CO.[24] Our work on the reactions of Zr^+ with CH_4 provided BDEs for Zr^+-CH, Zr^+-CH_2, and Zr^+-CH_3.[21] Bowers and co-workers have measured the binding energies of 1−7 H_2 molecules to Zr^+ using equilibrium methods.[25] Photodissociation was used by Ranatunga and Freiser to measure the $Zr^+-C_2H_2$ bond energy.[26] In addition, theoretical calculations have been performed for the BDEs of several species relevant to the present work: ZrH^+,[21,27−30] $Zr(H)_2^+$,[25,31] ZrC^+,[21] $ZrCH^+$,[21] $ZrCH_2^+$,[21,30,32,33] $ZrCH_3^+$,[21,34] $Zr(H)(CH_3)^+$ and $Zr(CH_4)^+$,[21,35] $Zr(CH_3)_2^+$ and $Zr(C_2H_6)^+$,[36] and $Zr(C_2H_2)^+$.[37]

In the present work, we measure several new BDEs by determining the endothermic thresholds for reactions of Zr^+ with the three hydrocarbons. We use a dc-discharge flow tube ion source to produce Zr^+ ions that are believed to be in the ^4F electronic ground state term.[23] Thus, the threshold measurements have few complexities associated with the presence of excited state ions.

One of the challenging problems in the study of alkane activation by transition metal ions is to determine reaction mechanisms. In contrast to work on first-row transition metal cations (mostly Fe^+, Co^+, and Ni^+), few detailed experimental and theoretical studies have been carried out to elucidate the mechanisms of second-row transition metal cations.[16,17,21,35,38] Nevertheless, it is clear that the mechanisms for alkane activation do vary with the identity of the metal ions, both from early to late and from first-row to second-row transition metal cations, as we have recently reviewed.[20] Here, we examine the likely mechanisms for reactions of Zr^+ and compare them to those for the first-row congener, Ti^+.[39−41]

Experimental Section

General Procedures. These studies are performed using a guided ion beam tandem mass spectrometer. The instrument and experimental methods have been described previously.[42,43] Ions, formed as described below, are extracted from the source, accelerated, and focused into a magnetic sector momentum analyzer for mass analysis. For these experiments, the ^{90}Zr isotope (51.5% natural abundance) is used. The ions are decelerated to a desired kinetic energy and focused into an octopole ion guide that radially traps the ions. While in the octopole, the ions pass through a gas cell that contains the neutral reactant at pressures where multiple collisions are improbable (<0.30 mTorr). Single-collision conditions were verified (with one exception noted below) by examining the pressure dependence of the cross sections measured here. The product ions and the reactant ion beam drift out of the gas cell, are focused into a quadrupole mass filter, and then are detected by a secondary electron scintillation detector. Ion intensities are converted to absolute cross sections as described previously.[42] Uncertainties in the absolute cross sections are estimated at ±20%.

To determine the absolute zero and distribution of the ion kinetic energy, the octopole is used as a retarding energy analyzer.[42] The uncertainty in the absolute energy scale is ±0.05 eV (lab). The full width at half-maximum (fwhm) of the ion energy distribution is 0.2−0.4 eV (lab). Lab energies are converted into center-of-mass energies using $E(\mathrm{CM}) = E(\mathrm{lab})\text{-}m/(m + M)$ where M and m are the masses of the ion and neutral reactants, respectively. At the lowest energies, the ion energies are corrected for truncation of the ion beam as described previously.[42] All energies referred to below are in the center-of-mass frame.

Ion Source. The ion source used here is a dc-discharge/flow tube (DC/FT) source described in previous work.[43] The DC/FT source utilizes a zirconium cathode held at 1.5−3 kV over which a flow of approximately 90% He and 10% Ar passes at a typical pressure of ~0.5 Torr. Ar^+ ions created in a direct current discharge are accelerated toward the zirconium cath-

Downloaded by CARLI CONSORTIUM on June 29, 2009
Published on May 23, 2003 on http://pubs.acs.org | doi: 10.1021/om030028u

(23) Sievers, M. R.; Chen, Y.-M.; Elkind, J. L.; Armentrout, P. B. *J. Phys. Chem.* **1996**, *100*, 54.
(24) Sievers, M. R.; Chen, Y.-M.; Armentrout, P. B. *J. Chem. Phys.* **1996**, *105*, 6322.
(25) Bushnell, J. E.; Kemper, P. R. van Koppen, P.; Bowers, M. T. *J. Phys. Chem.* **2001**, *105*, 2216.
(26) Ranatunga, D. R. A.; Freiser, B. S. *Chem. Phys. Lett.* **1995**, *233*, 319.
(27) Schilling, J. B.; Goddard, W. A., III; Beauchamp, J. L. *J. Am. Chem. Soc.* **1987**, *109*, 5565.
(28) Pettersson, L. G. M.; Bauschlicher, C. W., Jr.; Langhoff, S. R.; Partridge, H. *J. Chem. Phys.* **1987**, *87*, 481.
(29) Das, K. K.; Balasubramanian, K. *J. Mol. Spectrosc.* **1991**, *148*, 250.
(30) Siegbahn, P. E. M.; Blomberg, M. R. A.; Svensson, M. *Chem. Phys. Lett.* **1994**, *223*, 35.
(31) Das, K. K.; Balasubramanian, K. *J. Chem. Phys.* **1989**, *91*, 2433.
(32) Blomberg, M. R. A.; Siegbahn, P. E. M. *ACS Symp. Ser.* **1998**, *677*, 197.
(33) Bauschlicher, C. W., Jr.; Partridge, H.; Sheehy, J. A.; Langhoff, S. R.; Rosi, M. *J. Phys. Chem.* **1992**, *96*, 6969.
(34) Bauschlicher, C. W., Jr.; Langhoff, S. R.; Partridge, H.; Barnes, L. A. *J. Chem. Phys.* **1989**, *91*, 2399.
(35) Blomberg, M. R. A.; Siegbahn, P. E. M.; Svensson, M. *J. Phys. Chem.* **1994**, *98*, 2062.
(36) Rosi, M.; Bauschlicher, C. W., Jr.; Langhoff, S. R.; Partridge, H. *J. Phys. Chem.* **1990**, *94*, 8656.
(37) Sodupe, M.; Bauschlicher, C. W., Jr. *J. Phys. Chem.* **1991**, *95*, 8640.
(38) Perry, J. K. Ph.D. Thesis, Caltech, 1994.
(39) Sunderlin, L. S.; Armentrout, P. B. *J. Phys. Chem.* **1988**, *92*, 1209.
(40) Sunderlin, L. S.; Armentrout, P. B. *Int. J. Mass Spectrom. Ion Processes* **1989**, *94*, 149.
(41) van Koppen, P. A. M.; Bowers, M. T.; Haynes, C. L.; Armentrout, P. B. *J. Am. Chem. Soc.* **1998**, *120*, 5704.
(42) Ervin, K. M.; Armentrout, P. B. *J. Chem. Phys.* **1985**, *83*, 166.

Downloaded by CARLI CONSORTIUM on June 29, 2009
Published on May 23, 2003 on http://pubs.acs.org | doi: 10.1021/om030028u

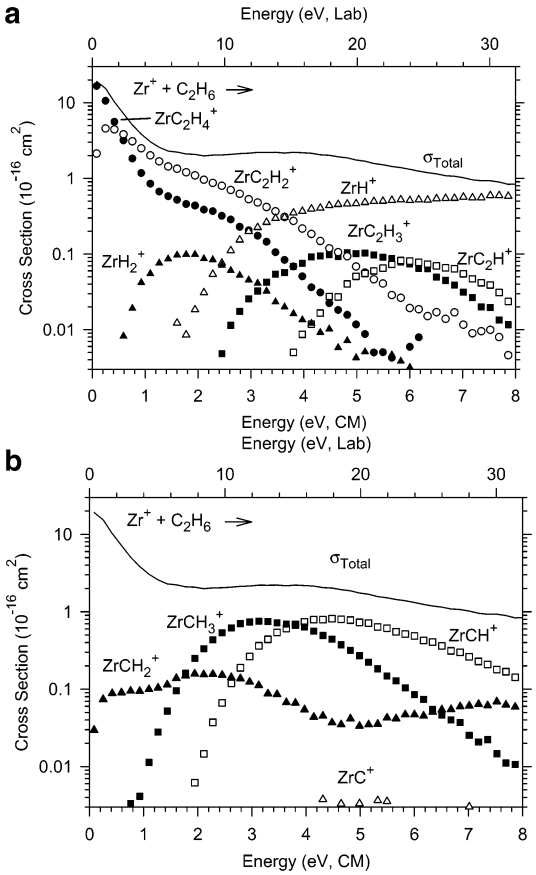

Figure 1. Cross sections for reactions of Zr^+ with C_2H_6 as a function of kinetic energy in the center-of-mass frame (lower axis) and laboratory frame (upper axis). Part a shows product channels in which the C−C bond remains intact, whereas part b shows product channels in which the C−C bond is cleaved. The full lines show the total cross section for all products.

ode, sputtering off atomic metal ions. The ions then undergo ~10^5 collisions with He and ~10^4 collisions with Ar in the meter long flow tube before entering the guided ion beam apparatus. Results obtained previously[23] indicate that the ions produced in the DC/FT source are exclusively in their a^4F ground state. This study determined that the electronic temperature is likely to be 300 ± 100 K, such that the average electronic energy of Zr^+ is 0.013 ± 0.004 eV.

Data Analysis. Previous theoretical[44] and experimental work[45] has shown that endothermic cross sections can be modeled using eq 1,

$$\sigma(E) = \sigma_0 \sum g_i (E + E_{el} + E_i - E_0)^n / E \qquad (1)$$

where σ_0 is an energy-independent scaling parameter, E is the relative translational energy of the reactants, E_{el} is the average electronic energy of the Zr^+ reactant (noted above), E_0 is the reaction threshold at 0 K, and n is a parameter that controls the shape of the cross section. The summation is over each ro-vibrational state of the neutral reactant having relative populations g_i and energies E_i. The various sets of vibrational frequencies used in this work are taken from the literature.[46]

Before comparison with the data, the model is convoluted over the neutral and ion kinetic energy distributions using previously developed methods.[42] The parameters E_0, σ_0, and n are then optimized using a nonlinear least-squares analysis in order to best reproduce the data. Reported values of E_0, σ_0, and n are mean values for each parameter from the best fits to several independent sets of data, and uncertainties are one standard deviation from the mean. The listed uncertainties in the E_0 values also include the uncertainty in the absolute energy scale and the uncertainty in the electronic energy of Zr^+.

Results

Cross sections for reaction of Zr^+ with the three small hydrocarbons are presented in the following sections. In some cases, these cross sections have been corrected for mass overlap between products ions having adjacent masses, but only where such corrections are unambiguous. Thermodynamic information for the stable and radical hydrocarbons required to interpret these results has recently been compiled.[18] The only additional values needed here are those for C_2H, C_3H_2, and c-C_3H_4, which have heats of formation at 0 K of 5.82 ± 0.03,[47] 5.61 ± 0.17 eV,[48] and 2.962 ± 0.026 eV.[49]

$Zr^+ + C_2H_6$. The reaction of zirconium cation with ethane yields the products listed in reactions 2−11. These are shown in Figures 1a and 1b.

$$Zr^+ + C_2H_6 \rightarrow ZrH^+ + C_2H_5 \qquad (2)$$

$$\rightarrow ZrH_2^+ + C_2H_4 \qquad (3)$$

$$\rightarrow ZrC^+ + CH_4 + H_2 \qquad (4)$$

$$\rightarrow ZrCH^+ + CH_3 + H_2 \qquad (5)$$

$$\rightarrow ZrCH_2^+ + CH_4 \qquad (6)$$

$$\rightarrow ZrCH_3^+ + CH_3 \qquad (7)$$

$$\rightarrow ZrC_2H^+ + 2\,H_2 + H \qquad (8)$$

$$\rightarrow ZrC_2H_2^+ + 2\,H_2 \qquad (9)$$

$$\rightarrow ZrC_2H_3^+ + H_2 + H \qquad (10)$$

$$\rightarrow ZrC_2H_4^+ + H_2 \qquad (11)$$

Figure 1a shows all product channels in which the C−C bond is retained. The dominant reaction of Zr^+ with ethane at low energies is dehydrogenation, reaction 11. The cross section for this process declines with increasing energy, consistent with an exothermic reaction having no barriers in excess of the energy of the reactants. This cross section declines approximately as

(43) Schultz, R. H.; Armentrout, P. B. *Int. J. Mass Spectrom. Ion Processes* **1991**, *107*, 29.
(44) Chesnavich, W. J.; Bowers, M. T. *J. Phys. Chem.* **1979**, *83*, 900.
(45) Armentrout, P. B. In *Advances in Gas-Phase Ion Chemistry*; Adams, N. G., Babcock L. M., Eds.; JAI: Greenwich, 1992; Vol. 1, pp 83−119.
(46) Shimanouchi, T. *Table of Molecular Vibrational Frequencies, Consolidated*; National Bureau of Standards: Washington, DC, 1972; Vol. I.
(47) Ervin, K. M.; Gronert, S.; Barlow, S. E.; Gilles, M. K.; Harrison, A. G.; Bierbaum, V. M.; DePuy, C. H.; Lineberger, W. C.; Ellison, G. B. *J. Am. Chem. Soc.* **1990**, *112*, 5750.
(48) Robinson, M. S.; Polak, M. L.; Bierbaum, V. M.; DePuy, C. H.; Lineberger, W. C. *J. Am. Chem. Soc.* **1995**, *117*, 6766.
(49) Dorofeeva, O. V.; Gurvich, L. V.; Jorish, V. S. *J. Phys. Chem. Ref. Data* **1986**, *15*, 437.

Downloaded by CARLI CONSORTIUM on June 29, 2009
Published on May 23, 2003 on http://pubs.acs.org | doi: 10.1021/om030028u

$E^{-0.5}$ from 0 to 0.2 eV, consistent with the Langevin−Gioumousis−Stevenson (LGS) collision cross section for ion−molecule collisions.[50] The magnitude of this cross section at these energies is 15% of the LGS cross section. Above 0.2 eV, the $ZrC_2H_4^+$ cross section drops more rapidly ($\sim E^{-1.9}$) as the $ZrC_2H_2^+$ product is formed. This indicates that the slightly endothermic double dehydrogenation, reaction 9, depletes the $ZrC_2H_4^+$ product. The total cross section declines as $E^{-1.2}$ from 0.2 to about 3 eV. Above 3 eV, both the $ZrC_2H_4^+$ and $ZrC_2H_2^+$ product cross sections begin to decline more rapidly. This is apparently caused by competition with the formation of ZrH^+ in reaction 2, as no other product has a cross section of sufficient intensity to account for the declines. The sum of the $ZrC_2H_4^+$, $ZrC_2H_2^+$, and ZrH^+ cross sections decreases smoothly, thereby indicating that these species likely share a common intermediate.

At higher energies, $ZrC_2H_3^+$ is formed in reaction 10. This species either must come from H atom loss from the $ZrC_2H_4^+$ product or could evolve from dehydrogenation of $ZrC_2H_5^+$. This latter product was looked for and not observed, such that it does not have a cross section exceeding 0.005 Å^2. It is possible that the $ZrC_2H_5^+$ species loses H_2 readily such that its cross section never reaches an appreciable magnitude. This hypothesis is consistent with the relative magnitudes of the $ZrC_2H_5^+$ and $ZrC_2H_3^+$ cross sections observed in the propane system (see below). The cross section for $ZrC_2H_3^+$ rises from an apparent threshold near 2.3 eV until near 5 eV, where it begins to fall off. This decline is largely attributable to further dehydrogenation to form ZrC_2H^+ in reaction 8.

One interesting minor product observed is ZrH_2^+, formed in reaction 3. This process competes directly with dehydrogenation to form $ZrC_2H_4^+$ in reaction 11. Clearly endothermic, this reaction reaches a maximum cross section close to the threshold observed for ZrH^+ formation. The ZrH_2^+ cross section does not reach a maximum at this energy because this species decomposes to ZrH^+, as this process corresponds to the overall formation of $ZrH^+ + H + C_2H_4$, which cannot occur until 3.56 ± 0.08 eV. Therefore, the ZrH_2^+ cross section must decline at this energy because the ZrH^+ channel depletes a common intermediate.

Figure 1b shows the products formed by cleavage of the C−C bond in ethane. The lowest energy product is the formation of $ZrCH_2^+$, indicating the neutral product must be methane, reaction 6. This product cross section rises from an apparent threshold near 0 eV, characteristic of an inefficient near-thermoneutral reaction or reaction over a barrier. The cross section rises until near 2 eV, then declines before rising again near 5 eV. This latter feature must correspond to $CH_3 + H$ products, which can begin at $D_0(CH_3-H) = 4.48$ eV above the threshold for reaction 6. The apparent threshold for this high-energy process provides another indication that reaction 6 must be near thermoneutral. The $ZrCH_3^+$ cross section rises from an apparent threshold below 1 eV, continues rising to near 3 eV, and then declines. The shape of the cross section indicates that $ZrCH_3^+$ loses H_2 to form $ZrCH^+$. A minor decomposition channel is H atom loss to form $ZrCH_2^+$, accounting for the high-energy feature in the $ZrCH_2^+$ cross section. The $ZrCH^+$ cross section rises from an apparent threshold near 2 eV and reaches a maximum near 4.5 eV, which we attribute to decomposition of the $ZrCH_3^+$ precursor to $Zr^+ + CH_3$, a process that can begin at $D_0(CH_3-CH_3) = 3.81$ eV. At higher energies, small amounts of ZrC^+ are also observed. The ZrC^+ cross section reaches a maximum of $\sim 4 \times 10^{-19}$ cm^2 and starts near 3 eV. On the basis of the energetics determined elsewhere,[21] this occurs by H_2 loss from $ZrCH_2^+$ in the overall reaction 4, which has a calculated threshold of 2.67 ± 0.11 eV, in good agreement with the apparent threshold.

In previous work on this system at thermal energies, Ranasinghe et al.[22] observed the dehydrogenation and double dehydrogenation processes, reactions 11 and 9, with a branching ratio of 77:23. No overall reaction efficiency was reported. Such a branching ratio is observed in our work (Figure 1a) at a kinetic energy of about 0.2 eV, which could indicate that the ICR study has kinetically excited ions or has not cooled the electronically excited states of Zr^+ completely. Similar conclusions have been drawn in comparing our results for similar reactions of Nb^+ and Rh^+ with those from Freiser and co-workers.[14,17]

$Zr^+ + C_3H_8$. The reaction of zirconium cation with propane yields a plethora of products, as formed in reactions 12−25. These cross sections are shown in Figure 2.

$$Zr^+ + C_3H_8 \rightarrow ZrH^+ + C_3H_7 \quad (12)$$

$$\rightarrow ZrH_2^+ + C_3H_6 \quad (13)$$

$$\rightarrow ZrCH^+ + C_2H_5 + H_2 \quad (14)$$

$$\rightarrow ZrCH_2^+ + C_2H_6 \quad (15)$$

$$\rightarrow ZrCH_3^+ + C_2H_5 \quad (16)$$

$$\rightarrow ZrCH_4^+ + C_2H_4 \quad (17)$$

$$\rightarrow ZrC_2H^+ + CH_3 + 2\,H_2 \quad (18)$$

$$\rightarrow ZrC_2H_2^+ + CH_4 + H_2 \quad (19)$$

$$\rightarrow ZrC_2H_3^+ + CH_3 + H_2 \quad (20)$$

$$\rightarrow ZrC_2H_4^+ + CH_4 \quad (21)$$

$$\rightarrow ZrC_2H_5^+ + CH_3 \quad (22)$$

$$\rightarrow ZrC_3H_2^+ + 3\,H_2 \quad (23)$$

$$\rightarrow ZrC_3H_4^+ + 2\,H_2 \quad (24)$$

$$\rightarrow ZrC_3H_6^+ + H_2 \quad (25)$$

The total cross section declines as $E^{-0.5}$ from 0.02 to 0.3 eV and has a magnitude of $(1.6 \pm 0.3) \times 10^{-14}$ cm^2 at 0.04 eV $\approx 3kT/2$ ($T = 298$ K). Both the energy dependence and the magnitude are consistent with the Langevin−Gioumousis−Stevenson (LGS) collision cross section for ion−molecule collisions.[50] The dominant products observed involve the loss of dihydrogen from the transient $ZrC_3H_8^+$ intermediate to form $ZrC_3H_x^+$ products, as shown in Figure 2a. The primary product in this sequence is $ZrC_3H_6^+$, formed by dehydrogenation

(50) Gioumousis, G.; Stevenson, D. P. *J. Chem. Phys.* **1958**, *29*, 294.

Downloaded by CARLI CONSORTIUM on June 29, 2009
Published on May 23, 2003 on http://pubs.acs.org | doi: 10.1021/om030028u

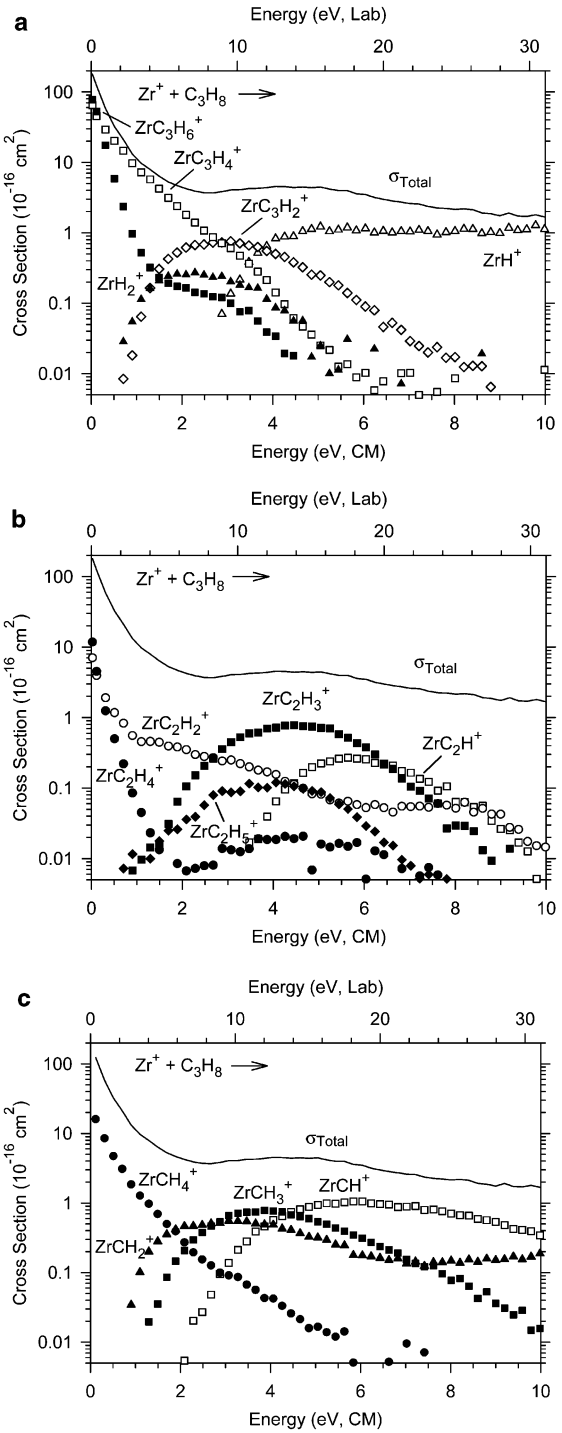

Figure 2. Cross sections for reactions of Zr^+ with C_3H_8 as a function of kinetic energy in the center-of-mass frame (lower axis) and laboratory frame (upper axis). Part a shows product channels in which the C−C bonds remain intact, whereas parts b and c show all product channels having $ZrC_2H_x^+$ and $ZrCH_x^+$ products, respectively. The full lines show the total cross section for all products.

of propane in reaction 25. This species accounts for 43% of the products at thermal energies (0.04 eV), but then falls off rapidly as E^{-3} above 0.3 eV. The magnitude of this product is limited by the efficiency of double dehydrogenation to form $ZrC_3H_4^+$ in reaction 24. Both processes 24 and 25 are exothermic, as indicated by cross sections that decline with increasing energy, showing no barriers in excess of the energy of the reactants. Double dehydrogenation accounts for 36% of all products at thermal energies (0.04 eV). As the energy is increased above 1.5 eV, the $ZrC_3H_4^+$ cross section drops more rapidly ($\sim E^{-2.8}$) as the $ZrC_3H_2^+$ product is formed. This indicates that the endothermic triple dehydrogenation, reaction 23, depletes the $ZrC_3H_4^+$ product. Above about 3.5 eV, the $ZrC_3H_6^+$, $ZrC_3H_4^+$, and $ZrC_3H_2^+$ product cross sections all begin to decline more rapidly. This is apparently caused by competition with the formation of ZrH^+ in reaction 12, as no other product has a cross section with sufficient intensity to account for the declines. The sum of the $ZrC_3H_6^+$, $ZrC_3H_4^+$, $ZrC_3H_2^+$, and ZrH^+ cross sections decreases smoothly, thereby indicating that these species likely share a common intermediate.

One reaction channel in direct competition with the major dehydrogenation processes is formation of ZrH_2^+, reaction 13. As shown in Figure 2a, formation of this product clearly exhibits a threshold. This cross section begins to decline close to the threshold observed for ZrH^+ formation; however, this cannot be because ZrH_2^+ decomposes to ZrH^+. This would be equivalent to the overall formation of $ZrH^+ + H + C_3H_6$, which cannot occur until 3.44 ± 0.08 eV. Therefore, as in the ethane system, the ZrH_2^+ cross section must decline at this energy because the ZrH^+ channel depletes a common intermediate.

Products formed by the cleavage of the C−C bond in the reaction of Zr^+ with propane are shown in Figures 2b and 2c. Of the various $ZrC_2H_x^+$ products, Figure 2b, two are formed in exothermic processes with no barriers in excess of the energy of the reactant. $ZrC_2H_4^+$, formed in reaction 21, is the most abundant of these, but accounts for only 7% of the products at thermal energies (0.04 eV). The cross section for this species rises again near 2 eV, which must correspond to the formation of $CH_3 + H$ instead of CH_4. The $ZrC_2H_4^+$ cross section declines rapidly at low energies, because dehydrogenation of this product to form $ZrC_2H_2^+$, reaction 19, is also exothermic. This product accounts for 4% of the reactivity at thermal energies (0.04 eV). This cross section rises slightly near 6 eV, and this must correspond to $CH_3 + H + H_2$ or $CH_4 + 2\ H$ products.

The cross sections for $ZrC_2H_3^+$ and $ZrC_2H_5^+$ begin near 1 eV. The $ZrC_2H_5^+$ cross section reaches a maximum near 4 eV but is never large because dehydrogenation of this product ion to form $ZrC_2H_3^+$ is energetically allowed with little excess energy. A secondary decomposition channel is H atom loss, which yields the higher energy feature in the $ZrC_2H_4^+$ cross section. The $ZrC_2H_3^+$ cross section rises until near 5 eV and then declines primarily because of dehydrogenation to ZrC_2H^+. A minor decomposition channel is probably H loss to form $ZrC_2H_2^+$, resulting in the second feature in that cross section beginning near 6 eV. The ZrC_2H^+ cross section rises from an apparent threshold near 3.5 eV and continues rising until near 6 eV, at which point it starts to decline because of further dissociation. The $ZrC_2H_x^+$ ($x = 5, 3, 1$) products can all decline starting at $D_0(CH_3-C_2H_5) = 3.78$ eV, because the $ZrC_2H_5^+$ species can decompose to $Zr^+ + C_2H_5$ starting at this energy. This may account for the gradual decline in the sum of these cross sections above ~5 eV.

Figure 2c shows ionic products containing Zr and a single carbon atom. Of these, only $ZrCH_4^+$ is formed in an exothermic process and accounts for 10% of all

products at thermal energies. (Possible contributions to this cross section from the isobaric ZrO^+ species, which could be formed by reactions with an O_2 contaminant,[24] were carefully checked for and verified to be absent.) This product competes directly with the exothermic formation of $ZrC_2H_4^+$ and has a magnitude comparable to the sum of the $ZrC_2H_4^+$ and $ZrC_2H_2^+$ cross sections. The $ZrCH_2^+$ cross section rises from a threshold somewhat below 1 eV. The cross section rises sharply and continues rising until near 4 eV, where it reaches a maximum because of competition with other channels and dissociation. A second feature in the $ZrCH_2^+$ cross section is also observed starting near 7 eV and can be attributed to neutral products of 2 CH_3 and/or C_2H_5 + H. $ZrCH_3^+$ rises from an apparent threshold near 1 eV and falls off near 4 eV largely because of dehydrogenation to form $ZrCH^+$. This secondary product rises from an apparent threshold near 2 eV and plateaus at higher energies.

In previous work on this system at thermal energies, Ranasinghe et al.[22] observed the single and double dehydrogenation processes, reactions 25 and 24, and the C−C bond cleavages, reactions 21 and 19, with a branching ratio of 8:86:3:3. No overall reaction efficiency was reported. Such a branching ratio is observed in our work (Figure 2) at a kinetic energy of about 0.9 eV, although we find very little $ZrC_2H_4^+$ at this energy. As noted above, we find a branching ratio of 43:36:7:4 at thermal energies, indicating less extensive decomposition than for the results of Ranasinghe et al.

Zr^+ + c-C_3H_6. Fourteen ionic products are observed in the reaction of Zr^+ with c-C_3H_6, reactions 26−39. Figure 3 shows cross sections for these as a function of kinetic energy.

$$Zr^+ + \text{c-}C_3H_6 \rightarrow ZrH^+ + \text{c-}C_3H_5 \quad (26)$$

$$\rightarrow ZrH_2^+ + \text{c-}C_3H_4 \quad (27)$$

$$\rightarrow ZrC^+ + H_2 + C_2H_4 \quad (28)$$

$$\rightarrow ZrCH^+ + H + C_2H_4 \quad (29)$$

$$\rightarrow ZrCH_2^+ + C_2H_4 \quad (30)$$

$$\rightarrow ZrCH_3^+ + C_2H_2 + H \quad (31)$$

$$\rightarrow ZrCH_4^+ + C_2H_2 \quad (32)$$

$$\rightarrow ZrC_2H^+ + H + CH_4 \text{ (or } H_2 + CH_3) \quad (33)$$

$$\rightarrow ZrC_2H_2^+ + CH_4 \quad (34)$$

$$\rightarrow ZrC_2H_4^+ + CH_2 \quad (35)$$

$$\rightarrow ZrC_3H^+ + H + 2\,H_2 \quad (36)$$

$$\rightarrow ZrC_3H_2^+ + 2\,H_2 \quad (37)$$

$$\rightarrow ZrC_3H_3^+ + H + H_2 \quad (38)$$

$$\rightarrow ZrC_3H_4^+ + H_2 \quad (39)$$

The total cross section declines as $E^{-0.5}$ from 0.03 to 0.3 eV and has a magnitude of $(2.0 \pm 0.4) \times 10^{-14}$ cm^2 at 0.04 eV $\approx 3kT/2$ (T = 298 K). Both the energy dependence and the magnitude are consistent with the

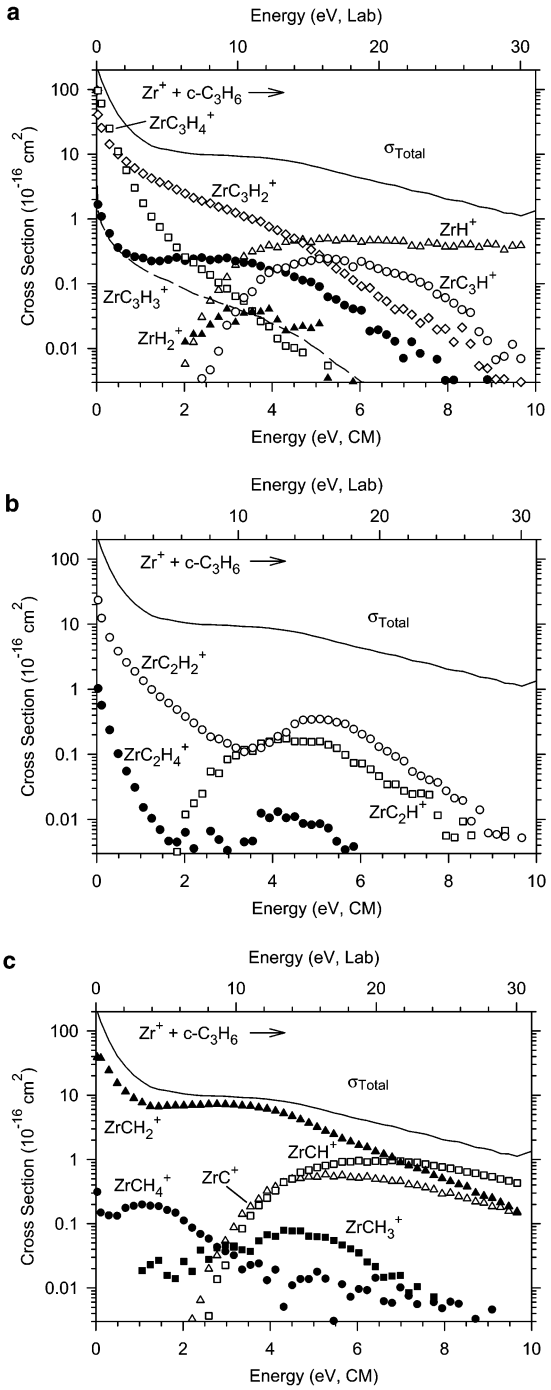

Figure 3. Cross sections for reactions of Zr^+ with c-C_3H_6 as a function of kinetic energy in the center-of-mass frame (lower axis) and laboratory frame (upper axis). Part a shows product channels in which the C−C bonds remain intact, whereas parts b and c show all product channels having $ZrC_2H_x^+$ and $ZrCH_x^+$ products, respectively. The dashed line in part a is the $ZrC_3H_2^+$ cross section scaled down by the probability of having a single ^{13}C. The full lines show the total cross section for all products.

Langevin−Gioumousis−Stevenson (LGS) collision cross section for ion−molecule collisions.[50] At low energies (below 2 eV), the $ZrC_2H_4^+$ cross section is dependent on the pressure of the cyclopropane reactant, indicating that an efficient, exothermic secondary reaction is occurring. The energy dependence observed clearly demonstrates that the secondary reaction is $ZrCH_2^+$ + c-C_3H_6 → $ZrC_2H_4^+$ + C_2H_4.

Downloaded by CARLI CONSORTIUM on June 29, 2009
Published on May 23, 2003 on http://pubs.acs.org | doi: 10.1021/om030028u

Downloaded by CARLI CONSORTIUM on June 29, 2009
Published on May 23, 2003 on http://pubs.acs.org | doi: 10.1021/om030028u

Figure 3a shows that the dehydrogenation channel, reaction 39, is the dominant process at low energies. This process constitutes 48% of the total cross section at 0.05 eV, but decreases rapidly as the energy increases. This is clearly because this product undergoes further dehydrogenation to yield $ZrC_3H_2^+$, reaction 37. Double dehydrogenation is also observed to be an exothermic process and constitutes 20% of the total cross section at thermal energies. An alternate decomposition pathway appears to be H atom loss, yielding the $ZrC_3H_3^+$ product, reaction 38. This reaction is slightly endothermic, although the cross section at the lowest energies is obscured by a contribution from a ^{13}C isotopomer of the much more intense $ZrC_3H_2^+$ product (Figure 3a). Further decomposition leads to the ZrC_3H^+ product, reaction 36. The magnitude and energy dependence of this cross section is consistent with formation by either H atom loss from $ZrC_3H_2^+$ or dehydrogenation of $ZrC_3H_3^+$. The cross sections for most of the $ZrC_3H_x^+$ species begin to decline more rapidly beginning at about 3−4 eV. This can be attributed to competition with formation of ZrH^+, reaction 26. At slightly lower energies, ZrH_2^+ is also formed and must correspond to elimination of a C_3H_4 neutral in reaction 27. On the basis of the thermodynamic information discussed below, the threshold for this process is consistent with formation of cyclopropene.

Unlike in the two alkane reaction systems, C−C bond cleavage reactions contribute significantly to the observed reactivity of Zr^+ with cyclopropane at low energies. Figure 3b shows that the formation of $ZrC_2H_2^+ + CH_4$ is exothermic and has no barriers with energies above the reactant asymptote. This process constitutes 12% of the total cross section at 0.05 eV. Beginning at about 3.5 eV, there is a distinct second feature in the $ZrC_2H_2^+$ cross section that can correspond to neutral products of $CH_3 + H$ (formed by H atom loss from a $ZrC_2H_3^+$ primary product) or possibly $CH_2 + H_2$ (formed by CH_2 loss from the $ZrC_3H_4^+$ primary product). This species can also lose a H atom to yield ZrC_2H^+, which might also be formed by methyl loss from $ZrC_3H_4^+$; however, the energy dependence observed is more consistent with the former path.

Formation of $ZrC_2H_4^+$ in reaction 35 is another C−C bond cleavage process and starts near 2 eV. This process competes directly with the much more favorable reaction 30, explaining its small magnitude. This cross section declines at energies above ~4 eV, probably because of dissociation into $Zr^+ + C_2H_4$, which can begin at 3.92 ± 0.03 eV $= D_0(C_2H_4-CH_2)$.

Starting about 0.3 eV, the C−C bond cleavage reaction 30 is the dominant process through much of the experimental energy range studied, Figure 3c. The $ZrCH_2^+$ cross section declines with energy and constitutes about 20% of all products observed at thermal energies. This cross section plateaus above 1 eV and then declines above about 3.5 eV, where this product can dissociate into $Zr^+ + CH_2$, $ZrCH^+ + H$ (reaction 29), or $ZrC^+ + H_2$ (reaction 28). These dissociation channels have thermodynamic thresholds of 3.92 ± 0.03, 2.33 ± 0.22, and 2.55 ± 0.11 eV (on the basis of the thermochemistry measured elsewhere[21]), respectively. The magnitude of the ZrC^+ cross section in this system is much larger than in the two alkane systems, consistent with the observation that its precursor, $ZrCH_2^+$, has the largest cross section magnitude in the c-C_3H_6 system. Another low-energy product observed is $ZrCH_4^+$, formed in reaction 32, which competes directly with reaction 34. $ZrCH_3^+$ is also observed, although its threshold is difficult to determine because of mass overlap with the much more intense $ZrCH_2^+$ cross section. Corrections for this overlap have been made in the $ZrCH_3^+$ cross section shown, but the uncertainty in the $ZrCH_3^+$ cross section below 3 eV is appreciable. Examination of the energetics of this reaction (see below) indicates that this product is formed along with C_2H_3.

Thermochemical Results

The energy dependences of the various cross sections are interpreted using eq 1. The optimum values of the parameters of eq 1 are listed for the ethane, propane, and cyclopropane systems in Tables 2−4, respectively. The thresholds can then be related to thermodynamic information assuming that this represents the energy of the product asymptote, an assumption that is usually correct for ion−molecule reactions because of the long-range attractive forces. Thus, eq 40 is used to derive the BDEs provided below, where RL is the reactant hydrocarbon.

$$D_0(Zr^+-L) = D_0(R-L) - E_0 \qquad (40)$$

Because our threshold analysis carefully includes all sources of reactant energy, the thermochemistry obtained is for 0 K.

ZrH^+. This product is formed in all three systems. Our most reliable value for $D_0(Zr^+-H)$, Table 1, is determined from the reactions of Zr^+ with H_2 and D_2.[23] This value is in reasonable agreement with high-level theoretical calculations.[21,27−30] Using this BDE, the predicted thresholds for the ZrH^+ products are 2.05 ± 0.08, 1.95 ± 0.08 to make 2-C_3H_7 and 2.00 ± 0.08 to make 1-C_3H_7, and 2.29 ± 0.08 eV for the C_2H_6, C_3H_8, and c-C_3H_6 systems, respectively. The thresholds measured for these processes, Tables 2−4, are within experimental error of these predictions. The small differences are apparently because of competition with more favorable dehydrogenation processes for each reaction system.

ZrC^+. Although ZrC^+ is observed in all three systems, it is a very minor product in reactions of the two alkanes. In contrast, formation of ZrC^+ in reaction 28 is quite prominent, clearly the result of the large cross section for $ZrCH_2^+$ formation. The bond energy for ZrC^+ has been measured previously from reactions of Zr^+ with CO,[24] Table 1. From this bond energy, the thresholds for formation of ZrC^+ in the ethane and cyclopropane systems are 2.67 ± 0.11 and 2.55 ± 0.11 eV, respectively. As noted above, the former value is in qualitative agreement with the apparent threshold observed in the ethane system, and the latter value is within experimental error of the measured threshold, Table 4. Given that the ZrC^+ BDEs obtained from CO and c-C_3H_6 are in good agreement, we take their weighted average as our overall best determination, $D_0(Zr^+-C) = 4.62 \pm 0.16$ eV (where the uncertainty is two standard deviations of the mean). This value is in excellent agreement with

Table 2. Optimized Parameters of Eq 1 for the $Zr^+ + C_2H_6$ System

reactants	products	σ_0	n	E_0, eV	$D_0(Zr^+-L)$, eV
$Zr^+ + C_2H_6$	$ZrH^+ + C_2H_5$	0.67 (0.15)	1.3 (0.2)	2.14 (0.13)	2.17 (0.13)
	$ZrH_2^+ + C_2H_4$	0.16 (0.02)	1.0 (0.2)	0.75 (0.08)	0.59 (0.08)
	$ZrCH^+ + CH_3 + H_2$	1.77 (0.32)	1.3 (0.2)	2.48 (0.13)	5.93 (0.13)
	$ZrCH_3^+ + CH_3$	1.03 (0.19)	1.7 (0.2)	1.39 (0.08)	2.42 (0.08)
	$ZrC_2H^+ + 2\ H_2 + H$	0.32 (0.05)	0.9 (0.2)	4.28 (0.12)	4.49 (0.12)
	$ZrC_2H_2^+ + 2\ H_2$	2.20 (0.44)	0.0 (0.2)	0.25 (0.15)	2.83 (0.15)
	$ZrC_2H_3^+ + H_2 + H$	0.16 (0.07)	1.5 (0.2)	2.48 (0.21)	3.62 (0.21)

Table 3. Optimized Parameters of Eq 1 for the $Zr^+ + C_3H_8$ System

reactants	products	σ_0	n	E_0, eV	$D_0(Zr^+-L)$, eV
$Zr^+ + C_3H_8$	$ZrH^+ + C_3H_7$	0.64 (0.22)	2.1 (0.3)	2.08 (0.15)	2.13 (0.15)
	$ZrH_2^+ + C_3H_6$	0.39 (0.08)	1.2 (0.3)	0.78 (0.13)	0.44 (0.13)
	$ZrCH^+ + C_2H_5 + H_2$	0.99 (0.23)	1.6 (0.2)	2.57 (0.11)	5.80 (0.11)
	$ZrCH_2^+ + C_2H_4 + H_2$	0.89 (0.07)	1.3 (0.2)	0.99 (0.10)	4.52 (0.10)
	$ZrCH_3^+ + C_2H_5$	0.85 (0.17)	1.7 (0.2)	1.44 (0.08)	2.34 (0.08)
	$ZrC_2H^+ + CH_3 + 2H_2$	0.60 (0.09)	1.5 (0.2)	3.63 (0.08)	4.60 (0.08)
	$ZrC_2H_3^+ + CH_3 + H_2$	0.72 (0.21)	1.6 (0.2)	1.70 (0.15)	3.86 (0.15)
	$ZrC_2H_4^+ + CH_3 + H$	0.048 (0.010)	0.8 (0.2)	2.44 (0.18)	2.84 (0.18)
	$ZrC_2H_5^+ + CH_3$[a]	0.54 (0.19)	1.9 (0.2)	1.41 (0.17)	2.37 (0.17)
	$ZrC_3H_2^+ + 3\ H_2$	1.23 (0.10)	1.6 (0.2)	1.01 (0.11)	5.45 (0.20)

[a] Analysis of the sum of the $ZrC_2H_5^+$ and $ZrC_2H_3^+$ cross sections.

Table 4. Optimized Parameters of Eq 1 for the $Zr^+ + c\text{-}C_3H_6$ System

reactants	products	σ_0	n	E_0, eV	$D_0(Zr^+-L)$, eV
$Zr^+ + c\text{-}C_3H_6$	$ZrH^+ + c\text{-}C_3H_5$	0.16 (0.13)	1.2 (0.2)	2.18 (0.24)	2.37 (0.24)
	$ZrH_2^+ + c\text{-}C_3H_4$	0.11 (0.08)	1.0 (0.2)	1.79 (0.37)	0.44 (0.37)
	$ZrC^+ + C_2H_4 + H_2$	0.77 (0.17)	1.3 (0.2)	2.78 (0.13)	4.49 (0.13)
	$ZrCH^+ + C_2H_4 + H$	1.11 (0.22)	1.5 (0.2)	3.08 (0.13)	5.21 (0.13)
	$ZrCH_4^+ + C_2H_2$			~0.0 (0.15)	0.95 (0.15)
	$ZrC_2H^+ + H + CH_4$	0.22 (0.07)	1.5 (0.2)	2.01 (0.17)	4.63 (0.17)
	$ZrC_3H^+ + 2\ H_2 + H$	0.71 (0.11)	0.8 (0.2)	3.21 (0.14)	
	$ZrC_3H_3^+ + H_2 + H$	0.25 (0.05)	1.1 (0.2)	0.97 (0.12)	4.10 (0.23)

Downloaded by CARLI CONSORTIUM on June 29, 2009
Published on May 23, 2003 on http://pubs.acs.org | doi: 10.1021/om030028u

the theoretical value of 4.60 eV calculated at the B3LYP level with the 6-311++G(3df,3p) basis on C and H and the Hay−Wadt relativistic effective core potential on Zr^+.[21]

$ZrCH^+$. As noted above, the mechanism for formation of $ZrCH^+$ in the alkane systems is dehydrogenation of the primary $ZrCH_3^+$ product and H atom loss from $ZrCH_2^+$ in the cyclopropane system. The thresholds obtained from the $ZrCH^+$ cross sections result in $D_0(Zr^+-CH)$ of 5.93 ± 0.13, 5.80 ± 0.11, and 5.21 ± 0.13 eV for the C_2H_6, C_3H_8, and c-C_3H_6 systems, respectively. The value obtained in our study of CH_4 and CD_4 reactivity provided BDEs of 5.98 ± 0.13 and 5.92 ± 0.20 eV.[21] Four of these values are in excellent agreement, so we take the weighted average of these values to obtain 5.89 ± 0.13 eV (where the uncertainty is two standard deviations of the mean) as our best value for $D_0(Zr^+-CH)$.

$ZrCH_2^+$. The dominant reactions in the methane and perdeuterated methane systems are dehydrogenation, slightly endothermic processes that were analyzed to provide $D_0(Zr^+-CH_2) = 4.60 \pm 0.04$ and 4.63 ± 0.04 eV, including zero-point energy corrections.[21] In the propane system, $ZrCH_2^+$ is not formed until about 1 eV, such that the neutral products in this case must correspond to $C_2H_4 + H_2$, a process that must occur through formation of the $ZrCH_4^+$ product. The measured threshold, Table 3, corresponds to $D_0(Zr^+-CH_2) = 4.52 \pm 0.10$ eV, quite consistent with the values derived from the methane system. We take the weighted average of all three values as our best value for $D_0(Zr^+-CH_2)$ and obtain 4.61 ± 0.05 eV (where the uncertainty is two standard deviations of the mean).

This BDE predicts that the formation of $ZrCH_2^+ + CH_4$ in the ethane system is exothermic by 0.6 eV, yet this reaction channel occurs very inefficiently at thermal energies and increases with increasing energy. This suggests that there is a barrier to this process. Alternative neutral products, $CH_3 + H$ or $CH_2 + H_2$, cannot occur until 3.91 ± 0.05 or 4.14 ± 0.06 eV, respectively, and must account for the high-energy feature in this cross section starting about 4.5 eV. In the cyclopropane system, formation of $ZrCH_2^+ + C_2H_4$ is exothermic by 0.7 eV and is quite efficient at thermal energies. This reflects the ability of Zr^+ to activate the strained C−C bonds of cyclopropane much more efficiently than those of the unstrained alkanes.

In our previous study, theoretical calculations indicate that the ground state of $ZrCH_2^+$ is $^2A'$ with a $^4B_2$ state lying 0.81 eV higher in energy. Given this excitation energy and the $D_0(Zr^+-CH_2)$ value determined above, formation of this latter state should have a threshold of 0.24, 0.37, and 0.12 ± 0.06 eV in the ethane, propane, and cyclopropane systems, respectively. Because formation of the quartet state is spin-allowed from $Zr^+(^4F)$ reactants, it is feasible that the threshold observed in the ethane system corresponds to this spin-allowed process. Further, it seems likely that in the cyclopropane system this spin-allowed reaction explains the large plateau observed in the $ZrCH_2^+$ cross section.

$ZrCH_3^+$ and $ZrC_2H_5^+$. In the methane system previously studied, values of 2.32 ± 0.16 and 2.27 ± 0.18 eV were obtained for $D_0(Zr^+-CH_3)$.[21] Here, the thresholds obtained for the $ZrCH_3^+$ cross sections in the C_2H_6 and C_3H_8 systems result in values of 2.42 ± 0.08 and 2.34 ± 0.08 eV, respectively. In the c-C_3H_6 system, the

Downloaded by CARLI CONSORTIUM on June 29, 2009
Published on May 23, 2003 on http://pubs.acs.org | doi: 10.1021/om030028u

uncertainty in the $ZrCH_3^+$ cross section is too large to interpret the energy dependence with any confidence. The apparent threshold is close to that expected for formation of $ZrCH_3^+ + C_2H_3$ at 1.60 ± 0.11 eV. The weighted average of the four reliable BDE values is 2.36 ± 0.10 eV (where the uncertainty is two standard deviations of the mean), which compares well with the theoretical value of 2.48 eV given by Bauschlicher et al.[34] This identifies this species as the zirconium methyl cation.

In the propane system, cleavage of the C−C bond yields $ZrC_2H_5^+$ in competition with $ZrCH_3^+$. Inspection of the data indicates that the threshold for process 22 is similar to that for reaction 16, Figures 2b and 2c. Analysis of the $ZrC_2H_5^+$ cross section is complicated because this product dehydrogenates at slightly higher energies to form $ZrC_2H_3^+$. Therefore, we analyzed the sum of the $ZrC_2H_5^+$ and $ZrC_2H_3^+$ cross sections. The results in Table 3 lead to $D_0(Zr^+-C_2H_5) = 2.37 \pm 0.17$ eV, essentially identical with $D_0(Zr^+-CH_3)$. This is comparable to results for the first-row congener of zirconium, where $D_0(Ti^+-C_2H_5) \approx D_0(Ti^+-CH_3)$.[9] It is possible that the ground state geometry of $ZrC_2H_5^+$ is not the zirconium ethyl cation but rather $HZr(C_2H_4)^+$, a hydrido-ethene complex.

Products of Dehydrogenation: $Zr(C_2H_x)^+$, $x = 2$ and 4, and $Zr(C_3H_x)^+$, $x = 2$, 4, and 6. Dehydrogenations of ethane and propane by Zr^+ are exothermic, indicating that $D_0(Zr^+-C_2H_4) > 1.34$ eV and that $D_0(Zr^+-C_3H_6) > 1.22$ eV. Loss of methane in the reaction with propane is also exothermic, which means that $D_0(Zr^+-C_2H_4) > 0.80$ eV. Somewhat more speculatively, we can model the exothermic part of the $ZrC_2H_4^+$ cross section in the propane system with a power law, subtract it from the experimental cross section, and analyze the endothermic feature, Table 3. This yields $D_0(Zr^+-C_2H_4) = 2.84 \pm 0.18$ eV, in agreement with the lower limits. In the cyclopropane system, an approximate threshold for $ZrC_2H_4^+ + CH_2$ formation is 2 eV, yielding $D_0(Zr^+-C_2H_4) \approx 1.9 \pm 0.3$ eV, but this channel is likely to be suppressed by competition with the much more favorable $ZrCH_2^+ + C_2H_4$ channel, leading to a lower limit on the bond energy.

Subsequent dehydrogenation of the $ZrC_2H_4^+$ product formed in the propane system is also exothermic, giving $D_0(Zr^+-C_2H_2) > 2.54$ eV. Double dehydrogenation of ethane to form $ZrC_2H_2^+$ is slightly endothermic, with a measured threshold of 0.25 ± 0.15 eV (Table 2), which can be converted to $D_0(Zr^+-C_2H_2) = 2.83 \pm 0.15$ eV, consistent with the lower limit obtained in the propane system. This BDE is somewhat greater than that measured by photodissociation[26] but in good agreement with the calculated value,[37] Table 1. It is also comparable with the value for $Zr^+-C_2H_4$ determined above, lending additional credence to both values. On the basis of this bond energy, the formation of $ZrC_2H_2^+ + CH_2 + H_2$ in the cyclopropane system should start at 2.83 ± 0.15 eV, in rough agreement with the onset of the high-energy feature in this cross section, Figure 3b.

Double dehydrogenation of propane is exothermic, indicating that $D_0(Zr^+-C_3H_4) > 2.86$ eV, presuming that C_3H_4 has a propyne structure. This seems likely given that double dehydrogenation of ethane is also a relatively efficient process and almost certainly forms an ethyne ligand. This BDE provides further experimental evidence that a Zr^+−ethyne bond energy of 2.83 eV is accurate. Dehydrogenation of cyclopropane to form $ZrC_3H_4^+$ is also exothermic and seems likely to retain the cyclic carbon skeleton given the observation that cyclopropene is eliminated in the competitive reaction 27. Triple dehydrogenation of propane to form $ZrC_3H_2^+$ is also observed as an endothermic process, as is formation of this species in an exothermic double dehydrogenation of cyclopropane. Here, the difficulty is assigning a likely structure to this ligand, although a reasonable possibility is the C=C=CH_2 biradical. Assuming this dissociation asymptote, the thermochemistry measured in the propane system provides a Zr^+=C_3H_2 BDE of 5.45 ± 0.20 eV, which is consistent with a lower limit of 4.88 eV provided by the exothermicity of the cyclopropane reaction. This double bond is somewhat stronger than that for Zr^+=CH_2 of 4.61 ± 0.05 eV. This is plausible, as the Zr−C double bond can be augmented by delocalization of the C−C π electrons into an empty dπ orbital on zirconium, thereby forming nearly a triple bond.

ZrH_2^+ and $ZrCH_4^+$. Two of the more interesting minor products observed in these systems are ZrH_2^+ and $ZrCH_4^+$, products that are not observed in the reactions of first-row transition metal cations with these hydrocarbons. The ZrH_2^+ product is formed in all three systems studied here with thresholds resulting in $D_0(Zr^+-H_2) = 0.59 \pm 0.08$, 0.44 ± 0.13, and 0.44 ± 0.37 eV in the ethane, propane, and cyclopropane systems, respectively. This good agreement demonstrates that cyclopropene is eliminated in the reaction with cyclopropane. We take the weighted average of all three values, 0.55 ± 0.13 eV (where the uncertainty is two standard deviations of the mean), as our best determination of this BDE. In the case of $ZrCH_4^+$ formed in the C_3H_8 system (Figure 2c), the reaction is exothermic, indicating that $D_0(Zr^+-CH_4) > 0.80 \pm 0.01$ eV. In the cyclopropane system, formation of $ZrCH_4^+$ appears to be exothermic or close to thermoneutral (see discussion above). The latter assumption would give $D_0(Zr^+-CH_4) = 0.95 \pm 0.15$ eV.

The key issue for these species is their structure, which can either be the inserted $Zr(H)_2^+$ and $Zr(H)(CH_3)^+$ species or the electrostatically bound molecular complexes, $Zr(H_2)^+$ and $Zr(CH_4)^+$. Bowers and co-workers have measured the binding of H_2 to Zr^+ and determined a bond energy of 0.63 ± 0.01 eV,[25] in good agreement with the present result. They assign this species to the inserted $Zr(H)_2^+$ species. This is confirmed by their theoretical calculations, which find a $Zr(H)_2^+$ ($^2B_1$) ground state bound by 0.72 eV at the B3LYP level (H−Zr−H bond angle = 111.6°) and a $Zr(H)_2^+$ ($^2A_1$) ground state bound by 0.67 eV at the MP2 level. Noninserted $Zr(H_2)^+$ geometries were also found on the quartet surface lying either 0.20 (B3LYP) or 0.42 (MP2) eV higher in energy.

In calculations conducted in our study of the methane system, we found that the global minimum on the $Zr^+ + CH_4$ surface was a $Zr(H)(CH_3)^+$ (^2A) species with a H−Zr−C bond angle of 102.2° calculated to lie 1.06 eV below the $Zr^+(a^4F) + CH_4$ ground state reactant asymptote. Blomberg et al.[35] calculate that $Zr(H)(CH_3)^+$ has a $^2A'$ ground state with a H−Zr−C bond angle of 108.7°.

Downloaded by CARLI CONSORTIUM on June 29, 2009
Published on May 23, 2003 on http://pubs.acs.org | doi: 10.1021/om030028u

They find that it lies below $Zr^+(a^4F) + CH_4$ by 0.53 eV, but they carefully consider zero-point energies and the limitations in their calculations and correct their binding energy to estimate that $Zr(H)(CH_3)^+$ is bound by 1.22 eV. Both calculations are in reasonable agreement with our experimental value of 0.95 ± 0.15 eV. The alternate geometry of a $Zr(CH_4)^+$ complex ($^2A_1$ ground state) was also considered and calculated to have a bond energy of 0.71 eV (0.45 eV before correction) by Blomberg et al. and 0.67 eV in our work.[21] Such a species is inconsistent with our observations in both the propane and cyclopropane systems. Our calculations[21] also verify that $(H)_2ZrCH_2^+$ and $(H_2)ZrCH_2^+$ species, although stable intermediates, lie even higher in energy than the $Zr(CH_4)^+$ species.

Overall, the comparison with theory shows that the ZrH_2^+ and $ZrCH_4^+$ products are most plausibly assigned to the covalently bound dihydride, $Zr(H)_2^+$, and hydridomethyl, $Zr(H)(CH_3)^+$, complexes. Experimentally, the simple fact that these species are observed provides further evidence for this assignment, a point that is discussed in the mechanisms section below.

Regardless of the structure of the ZrH_2^+ and $ZrCH_4^+$ species, the thermochemistry measured here can also be converted to $D_0(Zr^+-2H) = 5.02 \pm 0.13$ eV and $D_0[Zr^+-(H)(CH_3)] = 5.43 \pm 0.15$ eV. When these bond energy sums are combined with $D_0(Zr^+-H)$ and $D_0(Zr^+-CH_3)$, Table 1, one can also determine the second covalent bonds: $D_0(HZr^+-H) = 2.76 \pm 0.15$ eV, $D_0(HZr^+-CH_3) = 3.17 \pm 0.17$ eV, and $D_0[(CH_3)Zr^+-H] = 3.06 \pm 0.18$ eV. In all cases, the second bond is stronger than the first, a result that is similar to the calculations of Rosi et al.[36] for $D_0(H_3CZr^+-CH_3)$, where the second methyl bond is 0.3 eV stronger than the first.

$ZrC_2H_x^+$ ($x = 1$ and 3). Various ionic products having the formula $ZrC_2H_x^+$ are formed in the C_2H_6 and C_3H_8 systems. Those resulting from dehydrogenation ($x = 2$ and 4) or simple bond cleavage ($x = 5$) are discussed above. Subsequent dehydrogenation of the primary $ZrC_2H_5^+$ product yields both $ZrC_2H_3^+$ and ZrC_2H^+. The thresholds obtained for the former species in the reactions with C_2H_6 and C_3H_8 give $D_0(Zr^+-C_2H_3)$ of 3.62 ± 0.21 and 3.86 ± 0.15 eV, respectively. We adopt the weighted average value, 3.78 ± 0.24 eV, as our best value (where the uncertainty is two standard deviations of the mean). Note that this BDE is greater than that for the single bond in Zr^+-CH_3, 2.36 ± 0.10 eV, but less than the double bond of Zr^+-CH_2, 4.61 ± 0.05 eV. As discussed elsewhere,[9] transition metal ion bonds to vinyl can be strengthened by delocalization of the C−C π electrons to the metal center, i.e., a dative bond in addition to the covalent bond. For the early first-row transition metal cations (Ti^+, V^+, and Cr^+), where there is an empty orbital to accept these electrons, the bond to vinyl is 1.42 ± 0.35 eV stronger than the bond to methyl, the same as the enhancement here of 1.42 ± 0.26 eV.

ZrC_2H^+ is measured to have thresholds that yield $D_0(Zr^+-C_2H) = 4.49 \pm 0.12$, 4.60 ± 0.08, and 4.63 ± 0.17 eV in the ethane, propane, and cyclopropane systems, respectively. The very good agreement between the three values leads us to assign the weighted mean value of 4.57 ± 0.12 eV to $D_0(Zr^+-C_2H)$ (where the uncertainty is two standard deviations of the mean). This bond energy is much stronger than $D_0(Zr^+-CH_3)$ and comparable to $D_0(Zr^+-CH_2)$, suggesting it has double-bond character. Presuming that this species has a $Zr^+-C\equiv CH$ structure, this can occur by delocalization of both pairs of C−C π electrons into the dπ orbitals on Zr^+, in essence forming two dative bonds in addition to the covalent Zr−C single bond. This consideration predicts a linear structure.

$ZrC_3H_x^+$, $x = 1$ and 3. Minor products observed in the cyclopropane system are $ZrC_3H_x^+$, where $x = 3$ and 1, Figure 3a. At low energies, these cross sections are obscured by mass overlap and isotopomers of the other $ZrC_3H_x^+$ products that are orders of magnitude more intense. In addition, competition with these other products could shift the thresholds for $ZrC_3H_3^+$ and ZrC_3H^+ to higher energies. Thus, the thresholds for these products should be considered as upper limits. Analysis of the cross sections after correction for mass and isotope overlap yields the results in Table 4. The threshold for the $ZrC_3H_3^+$ product corresponds to $D_0(Zr^+-C_3H_3) \geq 4.10 \pm 0.23$ eV if dissociation yields a CH_2CCH structure (1.0 eV lower in energy than if the cyclic C_3H_3 isomer is produced), which implies nothing about the structure of the complex. This value is comparable to the BDE for $ZrC_2H_3^+$, which has a single covalent Zr−C bond augmented by π interactions. No heat of formation for C_3H is available, so the threshold determination cannot be converted to a bond energy.

Discussion

Reaction Mechanism. The activation of alkanes by transition metal cations is generally explained using an oxidative addition mechanism in which M^+ inserts into a C−H or C−C bond to form $R-M^+-H$ or $R'-M^+-CH_3$ intermediates.[1,5,20] Products can be formed by reductive elimination of small molecules such as H_2 and CH_4 at low energies and by metal−hydrogen or metal−carbon bond cleavage at high energies. The elimination processes can occur either by multicenter transition states or by rearrangement of the intermediate through β-H or β-CH_3 transfers to form $(H)_2M^+(C_xH_{2x})$ or $(CH_3)(H)M^+(C_xH_{2x})$ species, which then reductively eliminate H_2 or CH_4, respectively. This general mechanism has also been invoked to interpret experimental observations for the reactions of the first-row transition metal congener, Ti^+, with alkanes.[39−41] Detailed deuterium-labeling studies in the propane system indicate that dehydrogenation has a rate-limiting step of β-H transfer to form $(H)_2Ti^+(C_3H_6)$ or a multicenter transition state for elimination of H_2, whereas methane elimination is limited by reductive elimination of methane from a $(CH_3)(H)Ti^+(C_2H_4)$ intermediate.[41] Among the key issues in determining the detailed mechanism is the spin states of the reactant, intermediates, and products and the stabilities of two types of possible intermediates: (a) $R-M^+-H$ and $R'-M^+-CH_3$, and (b) $(H)_2M^+(C_xH_{2x})$ and $(CH_3)(H)M^+(C_xH_{2x})$.

The reactants in the present work have a quartet spin state, $Zr^+(^4F) + C_xH_{2x+2}$ (or c-C_3H_6) (^1A). Calculations indicate that the ground state of ZrH^+ is $^3\Delta$ or $^3\Phi$,[21,28,29] $ZrCH_3^+$ is ^3E,[21,34] $ZrCH_2^+$ is $^2A'$ or $^2A_1$,[21,32] $Zr(H)_2^+$ is $^2A_1$ or $^2B_1$,[31] and $Zr(H)(CH_3)^+$ is ^2A or $^2A'$.[21,35] All other primary products involve an alkene or alkyne bound to Zr^+. $Zr(C_2H_2)^+$ is calculated to have a $^2A_2$ ground state,[37]

Downloaded by CARLI CONSORTIUM on June 29, 2009
Published on May 23, 2003 on http://pubs.acs.org | doi: 10.1021/om030028u

indicating a metallacyclopropene structure. Calculations have not been performed for $Zr(C_2H_4)^+$, but comparisons with results for analogous complexes of Ti[37,51] suggest that it also has a doublet ground state. Thus, formation of the $ZrH^+ + R$, $ZrCH_3^+ + R'$, and $ZrC_2H_5^+ + CH_3$ products is spin-allowed, whereas formation of all other primary products is spin-forbidden from ground state reactants. It seems certain that the $R-Zr^+-H$, $R'-Zr^+-CH_3$, and metallacyclobutane intermediates should have doublet spin ground states, in direct analogy with $Zr(H)_2^+$ and $Zr(H)(CH_3)^+$. Likewise, the possible $(H)_2Zr^+(C_xH_{2x})$, $(CH_3)(H)Zr^+(C_xH_{2x})$, and $(H)_2Zr^+(c\text{-}C_3H_4)$ intermediates should have doublet ground states. In all three hydrocarbon systems, this indicates that there is a change in spin from quartet to doublet as the reactants evolve to products. Our calculated potential energy surfaces for the $Zr^+ + CH_4$ reaction indicate that this spin change occurs as the zirconium ion interacts strongly with the hydrocarbon to form the $H-Zr^+-CH_3$ intermediate.[21] All subsequent rearrangements and the formation of all products can then evolve along the doublet surface. It seems likely that the crossing between the quartet and doublet surfaces occurs in a similar location along the potential energy surfaces for the three systems studied here. On the basis of the present results, it appears that the spin conversion is fairly efficient in these systems, as the reactions occur with efficiencies of 15 (ethane), 100 (propane), and 100% (cyclopropane) at thermal energies.

As discussed above, our present experimental results coupled with theoretical calculations[21] indicate that the $H-Zr^+-CH_3$ intermediate is stable compared to the $Zr^+ + CH_4$ reactants. Similarly, calculations indicate that $Zr^+(CH_3)_2$ is stable compared to $Zr^+ + C_2H_6$ reactants.[36] Likewise we can conclude that all possible $R-Zr^+-H$ and $R'-Zr^+-CH_3$ intermediates should also be stable compared to the reactants because the R−H and R′−CH_3 bonds are no stronger than $H-CH_3$ and the replacement of the methyl group by a larger alkyl should only stabilize the intermediate further.

As noted above, there is strong competition observed between the formation of the thermodynamically favored products, e.g., $ZrC_2H_4^+ + H_2$, $ZrC_3H_6^+ + H_2$, and $ZrC_3H_4^+ + H_2$ with the $ZrH^+ + R$ products in the three hydrocarbon systems. This indicates that the latter channel is kinetically favored and that these reactions pass through a common intermediate. The $H-Zr^+-R$ intermediate is an obvious choice, as ZrH^+ formation can occur by simple bond cleavage at elevated kinetic energies, whereas H_2 elimination must occur by a more restricted transition state. Thus, the existence of this intermediate is not in question for Zr^+ reacting with any hydrocarbon. Likewise, the existence of CH_3-Zr^+-R' intermediates seems certain, as these lead to the primary $ZrCH_3^+$ and $ZrC_2H_5^+$ products observed in the ethane and propane systems. The comparable metallacyclobutane intermediate is also the only reasonable low-energy pathway to form $ZrCH_2^+ + C_2H_4$ in the cyclopropane system. The mechanisms responsible for the dehydrogenation and alkane elimination reactions observed at low energy are more difficult to determine and are discussed in the following sections.

(51) Bauschlicher, C. W., Jr.; Langhoff, S. R.; Partridge, H. In *Organometallic Ion Chemistry*; Freiser, B. S., Ed.; Kluwer: Dordrecht, 1995; pp 47−87.

Dehydrogenation of Ethane and Propane. Dehydrogenation of the alkanes can proceed by initial C−H bond activation to form $H-Zr^+-C_xH_{2x+1}$. This intermediate can then rearrange through a multicenter transition state in which a β-H interacts directly with the H on the metal to yield a $(H_2)Zr^+(C_xH_{2x})$ complex. Alternatively, the β-H first transfers to the metal to form $(H)_2Zr^+(C_xH_{2x})$, which then reductively eliminates H_2, again forming $(H_2)Zr^+(C_xH_{2x})$. In either case, this latter intermediate generally loses the H_2 ligand, as it is bound much less strongly than the alkene (BDEs of 0.54 vs 2.84 eV, Table 1). Indeed, this large difference in binding energies makes it implausible (although not impossible) that a significant amount of $Zr(H_2)^+$ could be generated by competitive loss of the alkene. It seems more likely that the alkene could be lost from a $(H)_2Zr^+(C_xH_{2x})$ intermediate, as alkene loss (although still thermodynamically disfavored) is a simple bond cleavage reaction and hence kinetically more favorable than H_2 elimination, which requires reductive elimination involving a tight transition state. Thus, the observation of ZrH_2^+ products in both the ethane and propane systems provides circumstantial evidence for the pathway involving the $(H)_2Zr^+(C_xH_{2x})$ intermediate.

The stability of the $(H)_2Zr^+(C_xH_{2x})$ intermediates can be understood by considering the electronic configuration of the $Zr(H)_2^+$ molecule, as calculated by Bushnell et al.[25] As noted above, they find a ground state of either $^2B_1$ (B3LYP) or $^2A_1$ (MP2). The valence molecular orbitals (MOs) are $1a_1$ and $1b_2$ Zr−H bonding; $1a_2$, $1b_1$, and $2a_1$ d-like nonbonding; a $3a_1$ s-like nonbonding; and $2b_2$ and $4a_1$ antibonding orbitals, although there is probably extensive s−d mixing in the a_1 MOs. The two possible ground states have $(1a_1)^2(1b_2)^2(1b_1)^1$ or $(1a_1)^2(1b_2)^2(2a_1)^1$ electronic configurations, such that both states have empty d-like nonbonding orbitals. These empty orbitals are good acceptors of electron density, allowing a strong dative bond with an alkene, thereby forming stable $(H)_2Zr^+(C_xH_{2x})$ intermediates. This is also illustrated by the calculated geometry of the $Zr(H)_2(H_2)^+$ complex,[25] in which an intact H_2 molecule is bound perpendicular to the plane of $Zr(H)_2^+$. It seems plausible that ethene would interact most strongly with the $^2B_1$ state of $Zr(H)_2^+$, as this allows effective σ donation from the π electrons on ethene into the empty $2a_1$ orbital along with π back-bonding from the singly occupied $1b_1$ orbital into the π^* antibonding MO on ethene. Calculations would be interesting in this regard. (It might be noted that similar electronic considerations hold for the $(CH_3)(H)Zr^+(C_xH_{2x})$ intermediates, as our calculations[21] of the electronic structure of $Zr(H)(CH_3)^+$ show the same qualitative behavior, taking into account the reduced symmetry, compared to $Zr(H)_2^+$.)

Alkane Elimination from Ethane and Propane. Two types of alkane elimination processes are observed for the alkanes studied here, formation of $ZrCH_2^+ + CH_4$ in the ethane system and of $Zr(C_2H_4)^+ + CH_4$ in the propane system. The former reaction is likely to follow the same type of mechanism as that elucidated theoretically for formation of $ZrCH_2^+$ in the methane system:[21] specifically, elimination of CH_4 from a $H-Zr^+-CH_2-CH_3$ intermediate or from a $H_3C-Zr^+-CH_2-H$ intermediate, both passing through four-center transition states. These processes probably account for the forma-

Downloaded by CARLI CONSORTIUM on June 29, 2009
Published on May 23, 2003 on http://pubs.acs.org | doi: 10.1021/om030028u

tion of $ZrCH_2^+$ at the lowest energies in the ethane system (Figure 1b). The thermochemistry measured here indicates that this reaction is exothermic (by 0.57 ± 0.06 eV); hence the shape of the cross section indicates there is a barrier to this process. This is presumably because the four-center transition state is more restricted when an alkyl group rather than an H atom is involved.

The formation of $Zr(C_2H_4)^+ + CH_4$ in the propane system is interesting, as this C−C bond activation process can be fairly efficient for many metal cations,[1,2] in particular, the late first-row transition metal cations. In analogy with the dehydrogenation process, it seems likely that this reaction occurs by initial C−C bond activation to form $H_3C-Zr^+-C_2H_5$, followed by a β-H shift to yield the $(CH_3)(H)Zr^+(C_2H_4)$ intermediate, which then reductively eliminates methane. The observation of the $Zr(H)(CH_3)^+$ product (Figure 2c) is taken as evidence for this latter intermediate, using arguments parallel to those for the analogous $(H)_2Zr^+(C_3H_6)$ intermediate. Alternatively, initial primary C−H bond activation to form $H-Zr^+-1\text{-}C_3H_7$ followed by a β-CH_3 shift yields the same $(CH_3)(H)Zr^+(C_2H_4)$ intermediate. These two pathways cannot be distinguished on the basis of the present experiments, although calculations suggest that β-alkyl migrations are higher energy pathways than β-H shifts.[52] If the former pathway is active, then the inefficiency of methane elimination (C−C bond cleavages account for only 21% of the total reactivity at thermal energies) can be explained by the relative amounts of initial C−H versus C−C bond activation. This is presumably controlled by the relative energies of the insertion transition state. If the latter pathway is active, then the relative efficiencies of the β-H versus β-CH_3 shifts are probably determining.

It is interesting to find that the branching between methane and ethene elimination, reactions 21 and 17, is nearly 50:50 at thermal energies. As the elimination of methane requires only 0.95 eV versus 2.84 eV for ethene loss, this again points to a more constrained pathway for methane elimination. This is strongly suggestive of the inserted intermediate, $(CH_3)(H)Zr^+(C_2H_4)$.

C−C Bond Activation of Cyclopropane. As noted above, activation of the C−C bond of cyclopropane generates the metallacyclobutane intermediate, $c\text{-}ZrC_3H_6^+$. Cleavage across the ring leads to $ZrCH_2^+(C_2H_4)$, which can then lose ethene readily. The reverse of this process, addition of the π bond of ethene across the Zr^+-CH_2 bond, can be examined to understand the forward reaction more readily. This process can be understood by using simple molecular orbital ideas originally developed for the activation of H_2 and CH_4 by metal oxide ions.[53] As discussed in detail elsewhere,[1,2] activation of covalent bonds at transition metal centers is most facile when the metal has an empty s-like valence orbital to accept the pair of electrons in the covalent bond, and when it has a pair of valence dπ-like electrons to donate into the antibonding orbital of the bond to be broken. In the calculations of Bauschlicher et al.,[32] the valence MOs of $ZrCH_2^+$ are $1a_1$ and $1b_1$ M−C bonding; $1a_2$, $1b_2$, and $2a_1$ d-like nonbonding; a $3a_1$ s-like nonbonding; and $2b_1$ and $4a_1$ antibonding orbitals. (Our calculations indicate that the molecule distorts from C_{2v} to C_s symmetry,[21] but the general nature of these orbitals remains largely unchanged.) For $ZrCH_2^+$, the most likely acceptor orbital is the $3a_1$ MO and the π-donor orbital is one of the nonbonding MOs. The ground state of $ZrCH_2^+$ is $^2A_1$ with a $(1a_1)^2(1b_1)^2(1a_2)^0(1b_2)^0(2a_1)^1(3a_1)^0$ electron configuration, and there is a low-lying $^2A_2$ state with a configuration of $(1a_1)^2(1b_1)^2(1a_2)^1(1b_2)^0(2a_1)^0(3a_1)^0$.[32] Note that neither of these states occupy the $3a_1$ acceptor orbital. Thus, the interaction of ground state $ZrCH_2^+$ with C_2H_4 is attractive and allows facile addition of the C−C π bond across the Zr−C bond to form the metallacycle.

Reactivity Differences between Zr^+ and Ti^+. The kinetic energy dependences of the reactions of Ti^+ (the first-row transition metal congener of Zr^+) with C_2H_6 and C_3H_8 have been studied previously.[40,41] The differences in the reactivity of Ti^+ and Zr^+ can be summarized fairly succinctly. First, the efficiency of the dehydrogenation processes differs dramatically between the two metals for propane. Reactions 24 and 25 are exothermic and efficient, occurring on nearly every collision. In contrast, the corresponding reactions in the Ti^+ systems are much less efficient. Although barrierless, the reaction occurs in only 18% of all collisions.[41] For ethane, the dehydrogenation probabilities at thermal energy are more similar: 11.5% for Ti^+ and 15% for Zr^+.[40] Second, exothermic elimination of methane from propane, reactions 21 + 19, is inefficient for Zr^+ (11% of all products) but occurs at thermal energies, and there is also the competitive elimination of ethene (10% of all products) at thermal energies. For Ti^+, the exothermic methane elimination accounts for only 2% of all products and no ethene loss is observed at any energies.[41] Third, subsequent dehydrogenation of primary products (forming species such as ZrC^+, $ZrCH^+$, ZrC_2H^+, $ZrC_2H_2^+$, $ZrC_2H_3^+$, ZrC_3H^+, $ZrC_3H_2^+$, $ZrC_3H_3^+$, and $ZrC_3H_4^+$) is pronounced in the zirconium systems. Analogous processes are observed in the titanium systems but are much less efficient.

Most of these differences in reactivity can be understood simply on the basis of differences in thermochemistry. The hydride and methyl BDEs of titanium and zirconium cations are similar; compare $D_0(Ti^+-H) = 2.31 \pm 0.11$ eV and $D_0(Ti^+-CH_3) = 2.22 \pm 0.03$ eV[9] with the values in Table 1. In contrast, the ZrC^+, $ZrCH^+$, and $ZrCH_2^+$ bonds are stronger than the titanium analogues by 0.75 ± 0.23 eV.[9] Likewise, the $Zr^+-C_2H_4$ BDE exceeds that for $Ti^+-C_2H_4$[54] by 1.3 ± 0.2 eV, and Sodupe and Bauschlicher[37] have calculated that $D_0(Zr^+-C_2H_2)$ is greater than $D_0(Ti^+-C_2H_2)$ by 0.9 eV. Similar results should hold for all other alkene and alkyne complexes. Thus, formation of all products but MH^+ and $M(alkyl)^+$ is energetically more favorable in the zirconium system by over 0.6 eV. This clearly explains the third difference noted above, the relative efficiency of the subsequent dehydrogenation processes. To a large extent, these energy differences also explain the first two points, the differences in the reaction efficiencies with propane. Dehydrogenation of the alkanes by Ti^+ is energetically

(52) Yi, S. S.; Blomberg, M. R. A.; Siegbahn, P. E. M.; Weisshaar, J. C. *J. Phys. Chem.* **1998**, *102*, 395.
(53) Clemmer, D. E.; Aristov, N.; Armentrout, P. B. *J. Phys. Chem.* **1993**, *97*, 544.
(54) Sievers, M. R.; Jarvis, L. M.; Armentrout, P. B. *J. Am. Chem. Soc.* **1998**, *120*, 1891.

more costly than when induced by Zr^+, as is methane elimination from propane. Dehydrogenation and demethanation of propane by both metal cations are exothermic and have no barriers in excess of the energy of the reactants; hence the order of magnitude difference in efficiencies for these processes requires additional considerations.

As discussed previously,[41] the inefficiency of the reactions of Ti^+ with propane has been attributed to intermediates that lie only slightly below the energy of the reactants and the need to couple from a quartet reactant surface to a doublet intermediate surface. The most likely difference with Zr^+ is that the spin−orbit coupling necessary to mix the quartet and doublet surfaces in the entrance channel should be more effective for the heavier metal. A small contributor to these differences is that the lowest-lying doublet state of the atomic ion is lower in energy for Zr^+: the excitation energy of the ^2D ($5s^14d^2$) state of Zr^+ is 0.546 eV,[55] compared to the ^2F ($4s^13d^2$) state of Ti^+, which lies 0.593 eV above the ground state, and the ^2D state, which lies 1.082 eV above the ground state.[56] The ability of Zr^+ to form stronger multiple bonds (noted above) should also influence the relative stability of intermediates such as $H-M^+-R$, $R'-M^+-CH_3$, $(H)_2M^+(C_xH_{2x})$, and $(CH_3)(H)M^+(C_xH_{2x})$.

Conclusion

Ground state Zr^+ ions are found to be very reactive with C_2H_6, C_3H_8, and c-C_3H_6 over a wide range of kinetic energies. Efficient dehydrogenation is observed at low energies in all three reaction systems, whereas alkane elimination is nearly absent in the ethane system and moderate for propane. C−C bond activation of the strained cyclopropane ring, however, is quite facile and leads to ethene elimination as a dominant reaction channel. At high energies, the dominant process in the ethane, propane, and cyclopropane systems is C−H bond cleavage to form $ZrH^+ + R$, although there are also appreciable contributions from $ZrCH_3^+$, $ZrC_2H_5^+$, and products that result from dehydrogenation of these primary products, $ZrCH^+$ and $ZrC_2H_3^+$. The endothermic reaction cross sections observed in all three systems are modeled to yield 0 K bond dissociation energies for several Zr−ligand cations, as summarized in Table 1. Reasonable agreement is found for these values compared with previous experimental and theoretical work. Lower limits to Zr^+−alkene and Zr^+−alkyne BDEs are established by the observation of exothermic dehydrogenation reactions.

Possible mechanisms for the reactions of Zr^+ with these hydrocarbons are discussed in some detail. A key observation in the present system is the formation of ZrH_2^+ and $ZrCH_4^+$ species, proposed to be the covalently bound dihydride and hydrido-methyl complexes. These considerations suggest that the mechanisms of Zr^+ involve initial C−H or C−C bond activation followed by rearrangements to form $(H)(R)Zr^+$(alkene) intermediates. When compared to Ti^+, the first-row transition metal congener, Zr^+ is found to be much more reactive. This can be attributed to much stronger π bonds for the second-row metal ion and to more efficient coupling between surfaces of different spin.

Acknowledgment. This research is supported by the National Science Foundation, Grant No. CHE-0135517. We thank Sae-Young Shin and D. L. Steele for helping to acquire some of the data.

OM030028U

(55) Moore, C. E. *Atomic Energy Levels*; Natl. Stand. Ref. Data Ser., Natl. Bur. Stand. (NSRDS-ZRS) 1971, *35* Vol. II.

(56) Sugar, J.; Corliss, C. *J. Phys. Chem. Ref. Data* **1985**, *14*, 1, Suppl. 2.

Downloaded by CARLI CONSORTIUM on June 29, 2009
Published on May 23, 2003 on http://pubs.acs.org | doi: 10.1021/om030028u